

This article was downloaded by:

On: 23 January 2011

Access details: *Access Details: Free Access*

Publisher *Taylor & Francis*

Informa Ltd Registered in England and Wales Registered Number: 1072954 Registered office: Mortimer House, 37-41 Mortimer Street, London W1T 3JH, UK



## International Journal of Polymeric Materials

Publication details, including instructions for authors and subscription information:

<http://www.informaworld.com/smpp/title~content=t713647664>

### Crystallization Phenomena

A. Peterlin<sup>a</sup>

<sup>a</sup> Institute for Materials Research, Polymers Division, National Bureau of Standards, Washington, DC

**To cite this Article** Peterlin, A.(1979) 'Crystallization Phenomena', International Journal of Polymeric Materials, 7: 1, 1 — 28

**To link to this Article:** DOI: 10.1080/00914037908077912

**URL:** <http://dx.doi.org/10.1080/00914037908077912>

PLEASE SCROLL DOWN FOR ARTICLE

Full terms and conditions of use: <http://www.informaworld.com/terms-and-conditions-of-access.pdf>

This article may be used for research, teaching and private study purposes. Any substantial or systematic reproduction, re-distribution, re-selling, loan or sub-licensing, systematic supply or distribution in any form to anyone is expressly forbidden.

The publisher does not give any warranty express or implied or make any representation that the contents will be complete or accurate or up to date. The accuracy of any instructions, formulae and drug doses should be independently verified with primary sources. The publisher shall not be liable for any loss, actions, claims, proceedings, demand or costs or damages whatsoever or howsoever caused arising directly or indirectly in connection with or arising out of the use of this material.

# Crystallization Phenomena†

A. PETERLIN

*Institute for Materials Research, Polymers Division, National Bureau of Standards  
Washington, DC 20234*

*(Received February 13, 1978)*

The minimum requirement of the free enthalpy increase for the formation of any type of critical size nucleus determines the probability for the nucleation from supercooled melt or solution and for the subsequent crystal growth. The minimum demand decreases as the inverse square of the supercooling. This yields a rapid increase of the nucleation and growth rate with decreasing temperature. On the other hand, the viscous resistance of the melt or solution to the chain transfer from the liquid to the crystalline phase increases with the temperature approaching that of the glass transition. Both effects together yield a maximum of the nucleation and growth rates at a finite supercooling with a subsequent drastic drop at a higher supercooling. The extension and alignment of the polymer chains in the liquid by applied mechanical forces lowers the entropy and to some extent also the enthalpy of the liquid state, thus raising the equilibrium melting temperature of the system and increasing the effective supercooling. As a consequence the rate of nucleation and crystal growth is drastically increased. Moreover, the shape of the primary nuclei becomes substantially linear with orientation in the main strain direction. Since these linear elements carry most of the applied load or stress, the rest of the liquid can relax to such an extent that by epitaxial overgrowth the macromolecules are able to be deposited in more or less conventional lamellae perpendicular to the stress. This yields the shish-kebab structure in the stirred or sonicated solutions and the cylindrical structure in hard elastomers solidified from the extruded melt.

## INTRODUCTION

The last decades have convincingly demonstrated that the mechanical properties of polymer solids depend not only on the chemical structure of the macromolecule but just as much on the morphology of the solid state of the polymer which can be modified over wide limits by the mechanical and thermal treatment. Purely amorphous polymers need cross-links in order to retain their shape in the rubbery state which is actually a supercooled liquid with a very high viscosity. In semicrystalline polymers the crystals act as cross-links up to

---

†Presented at a Symposium on "Flow-Induced Crystallization" at the Midland Macromolecular Institute, August 22-26, 1977, R. L. Miller, Chairman.

their melting point which is substantially above the glass transition temperature of the amorphous component. The ordering of crystals by the melt extrusion or by the drawing of the solid polymer creates new structures which, depending on the connections between the crystals, vary between the hard elastomers and rigid fibers. The range of the axial elastic modulus is about four decades, from a very small fraction up to about 50% of the elastic modulus of the chain in the crystal lattice.

The ability to crystallize depends on the regularity of the polymer chain: the head-to-tail arrangement of identical mers, the stereoregularity, the small and regular side groups. An ideal system is the linear, unbranched polyethylene (PE) with the perfectly regular backbone. It crystallizes extremely fast from the melt or solution in folded-chain lamellae with an orthorhombic crystal lattice. It is certainly the most studied polymer as far as the nucleation, crystallization kinetics, and morphology are concerned. In that which follows most of the material reported will apply to PE although with proper modification it is directly applicable to other crystallizable polymers.

In discussing the crystallization phenomena we shall purposely omit the treatment of different morphologies which develop from the primary nucleus in solutions of widely varying concentration, in melts and solutions at different supercoolings, and at different molecular weight averages and under different cooling conditions, as, for instance, hollow pyramids, dendrites, axialites, spherulites, cylindrites, and transcrystalline structures. We shall instead concentrate on the basic thermodynamics involved in the homogeneous and heterogeneous nucleation, the role of the nucleation in crystal growth, and the modification of the enthalpy and entropy changes by the forces applied to the melt or solution either by the straining or flow with a finite gradient.

Since the uniaxial force field introduces an anisotropy of the polymer chain orientation and extension, this effect is reflected also in the crystalline superstructure of the solidified polymer. The nuclei grow to an extreme linear shape (row nuclei) which dominates the resulting morphology. The spherulites are modified to cylindrites and shish-kebab structures. But the details of their formation and morphology will be so much discussed by other speakers of this Symposium that they need to be mentioned only marginally in this introduction to the crystallization phenomena. Very much the same applies to the molecular details of the crystallization of a network where the deposition of each chain in the crystal lattice is limited by the fixation of its ends in the cross-links of the network.

## **HOMOGENEOUS NUCLEATION<sup>1,2</sup>**

At the phase transition from the solution or melt to the crystalline solid state,

or vice versa, the free enthalpy  $G$  per unit mass of both phases is equal,  $G_e = G_l$ . At any temperature the net rate of the transformation from one phase into the other one is an exponential function of the change  $\Delta G_f = G_l - G_e$

$$dm/dt = dm_{lc}/dt - dm_{cl}/dt = (kT/h)\rho A d[\exp(\Delta G_f/kT) - \exp(-\Delta G_f/kT)] \quad (1)$$

where  $h = 6.63 \times 10^{-34} J$  is the Planck constant, the ratio  $kT/h = 6.1 \times 10^{12} s^{-1}$  at  $20^\circ C$  is the number of attempts of the molecule per second to cross the energy barrier between the liquid and crystalline phases,  $\rho$  is the density of the crystalline material,  $d$  is the thickness of the deposited molecules, and  $A$  is the area of the interface between the two phases. The mass transport  $dm_{lc}/dt$  corresponds to crystallization and  $dm_{cl}/dt$  to melting or to dissolution. Both transports go on at the same time although at different rates as soon as  $\Delta G_f$  differs from zero. For positive values of  $\Delta G_f$  the crystallization prevails over the melting and for negative values the melting prevails. One sees that at the exact thermodynamic equilibrium no net crystallization, melting, or dissolution will take place. One needs a driving force, i.e. an excess of the free enthalpy of the liquid phase over that of the crystalline phase in order to let the crystallization process go on at a measurable pace.

In a very wide range of temperature one has

$$\Delta G_f = \Delta H_f T \Delta T / T_m^2 \quad (2)$$

or even better<sup>3</sup>

$$\Delta G_f = 2\Delta H_f T \Delta T / T_m(T + T_m) \quad (2b)$$

The free enthalpy of melting is roughly proportional to the supercooling  $\Delta T = T_m - T$ . Here the equilibrium melting temperature

$$T_m = \Delta H_f / \Delta S_f \quad (3)$$

and the specific heat of fusion or dissolution  $\Delta H_f$  apply to the phase transformation by the melting or dissolution of an infinitely large crystal into a fully relaxed liquid. The change of the entropy  $\Delta S_f$  equals the change from the completely randomized melt or solution ( $S_l$ ) to the ideally ordered crystal ( $S_c$ ).

The situation is complicated by the crystal-amorphous interface  $A$  with a specific surface free enthalpy  $\sigma$  as a consequence of the differences of forces between the molecules in both phases caused by the different packing and packing density. The contribution to  $\Delta G_f$  matters more with a smaller volume  $V$  of the crystalline phase. This is particularly so at the beginning of the crystallization when the first crystal nuclei are formed.

In the formation of a nucleus one gains  $\rho_c V \Delta G_f$  and needs  $A\sigma$  for the surface so that the total change of the free enthalpy turns out to be

$$\Delta g_f = -\rho_c V \Delta G_f + A\sigma \quad (4)$$

The shape anisotropy of linear macromolecules suggests the parallel packing of chains into a narrow bundle with the lateral width  $a$  and height  $c$ . In order to simplify the issue, let us assume that the bundle has a square cross-section. The surface free enthalpy will be  $\sigma$  at the rectangular side planes parallel to the chains and  $\sigma_e$  at the square end planes perpendicular to the chains. For such a nucleus one obtains

$$\Delta g_f = -\rho_c a^2 c \Delta G_f + 4ac\sigma + 2a^2\sigma_e \quad (4a)$$

This value increases with increasing  $a$  and  $c$  up to a saddle point at  $a^*$  and  $c^*$  beyond which it steadily decreases, cf. Figure 1. The saddle point is determined by

$$\partial \Delta g_f / \partial a = -2\rho_c a^* c^* \Delta G_f + 4c^* \sigma + 4a^* \sigma_e = 0$$

and

$$\partial \Delta g_f / \partial c = -\rho_c a^{*2} \Delta G_f + 4a^* \sigma = 0$$

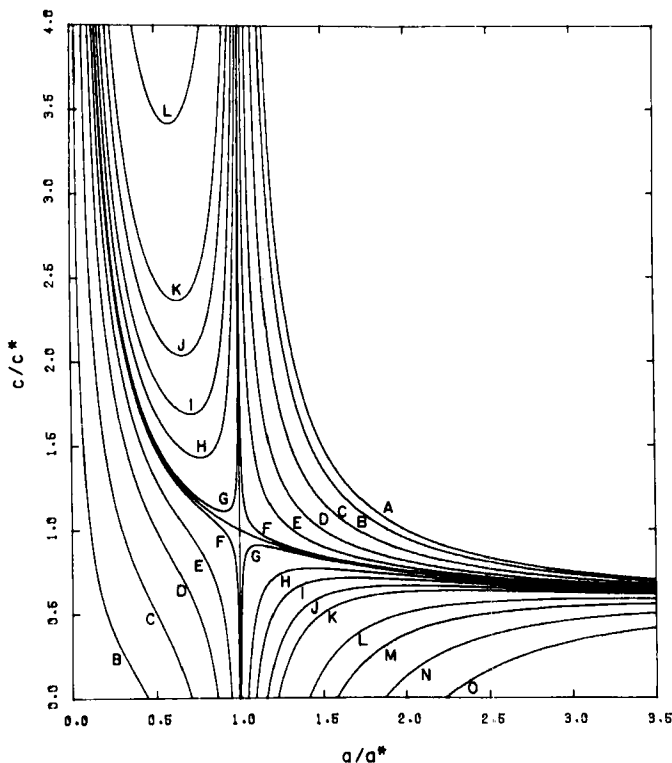


FIGURE 1 Free enthalpy surface,  $\Delta g_f$ , as a function of nucleus size,  $a$  and  $c$ , in coordinates relative to those of the saddle point ( $\Delta g_f^*$ ,  $a^*$ , and  $c^*$ ). The contours of constant free enthalpy ( $\Delta g_f/\Delta g_f^*$ ) are: A, 0.0; B, 0.2; C, 0.5; D, 0.75; E, 0.9; F, 0.99; G, 1.01; H, 1.1; I, 1.2; J, 1.35; K, 1.5; L, 2.0; M, 2.5; N, 3.5; O, 5.0. Courtesy of R. L. Miller.

A nucleus with dimensions

$$a^* = 4\sigma/\rho_c\Delta G_f \quad (5)$$

and

$$c^* = 4\sigma_e/\rho_c\Delta G_f \quad (5a)$$

has the minimum excess free enthalpy

$$\begin{aligned} \Delta g^*_f &= 32\sigma^2\sigma_e/(\rho_c\Delta G_f)^2 \\ &= (8\sigma^2\sigma_e/\rho_c^2) T_m^2(T + T_m)^2/T^2\Delta H_f^2(\Delta T)^2 \end{aligned} \quad (6)$$

required for the passing over the saddle point to the descending part of the free enthalpy surface of the crystal nucleus. This means that any increase of dimensions  $a$  and  $c$  beyond  $a^*$  and  $c^*$  will decrease the free enthalpy content of the nucleus. Such a nucleus will grow spontaneously while smaller nuclei will have a tendency to return to the amorphous phase which lowers their free enthalpy content. A free enthalpy surface for a nucleus is shown in Figure 1, in coordinates relative to the coordinates of the saddle point given by Eqs. (6) and (5).

The factor 32 in Eq. (6) corresponds to a square cross-section of the nucleus. If one assumes a shape with the cross-section commensurate to the basal plane of the PE unit cell, one obtains 30.2. A circular cross-section would yield 25.1. These differences are not exceedingly high but they influence the numerical values of parameters derived from an analysis of the experimental data on nucleation. One obtains an idea about the order of magnitude of the effects involved by calculating values of  $a^*$ ,  $c^*$ ,  $\Delta g^*_f$ ,  $\Delta g^*_f/kT$ , and  $\exp(-\Delta g^*_f/kT)$  with the parameters derived from the experimental data. If one takes the nucleation experiments<sup>4,5</sup> on droplets of molten PE at 359.8 K with  $\Delta T = 58$  K yielding  $\sigma_e = 93$  erg/cm<sup>2</sup> on the basis of assumptions of  $\sigma = 13.7$  erg/cm<sup>2</sup>,  $T_m = 417.8$  K,  $\Delta H_f = 2.9 \times 10^9$  erg/g,  $\rho_c = 1$  g/cm<sup>3</sup>, and a factor 30.2 one obtains 14.7 Å, 99.9 Å,  $3.73 \times 10^{-12}$  erg/g, 77.8, and  $1.51 \times 10^{-34}$ , respectively. With the factor 32, these values change to 14.7 Å, 99.9 Å,  $4.0 \times 10^{-12}$  erg/g, 82.5, and  $1.55 \times 10^{-36}$ , respectively. There is no substantial difference in  $a^*$  and  $c^*$  but the difference in  $\exp(-\Delta g^*_f/kt)$  amounting to a factor of 100 is quite conspicuous. These data demonstrate very convincingly that by a very small modification of the parameters one can shift appreciably the calculated values in order to achieve a better fit with the experimental data.

Since the dimensions of the critical nucleus are inversely proportional to the excess free enthalpy  $\Delta G_f$ , which increases almost linearly with the supercooling, one has a similarly inverse proportionality of  $a^*$  and  $c^*$  with  $\Delta T$ . The larger the supercooling, the thinner and shorter the critical nucleus and vice versa.

The ratio of  $a^*$  and  $c^*$  equals the ratio of  $\sigma$  and  $\sigma_e$ . The surface free enthalpy  $\sigma$  for the interface between the crystal and the melt or solution is between 10 and 15 erg/cm<sup>2</sup>. The value of  $\sigma_e$ , however, depends very much on the special type

of crystallization: folded-chain crystals, fringed-micelle crystals, or extended-chain crystals. This matter was mainly investigated in the case of linear polyethylene. The results will be briefly summarized as follows.

The *folds* contain mainly gauche conformations instead of the trans conformations of the ideal crystal lattice. For each gauche conformation one needs an additional free enthalpy amount of about 0.5 kcal/mol = 2100 J/mol. If each fold has  $n$  gauche conformations, the surface free enthalpy is increased by  $9.5n$  erg/cm<sup>2</sup>. With  $n$  about 6 one would have  $\sigma_e$  between 70 and 75 erg/cm<sup>2</sup>. The ratio of  $c^*$  to  $a^*$  is expected to be about  $n + 1$ . The nuclei are narrow, long parallelepipeds or cylinders.

The free enthalpy increase associated with the end face of a *fringed-micelle* crystal is much larger. It is not caused by an increase of the energy but by a substantial reduction of the entropy.<sup>6,7</sup> Forcing the molecules of, let us say, 2,000 lattice element lengths to participate at a fixed location reduces their conformational probability, i.e. their entropy, by about 3.5 k at each surface. The inaccessibility of the volume occupied by the crystal adds another reduction of about 4 k. The reduced volume available for molecular vibrations caused by the presence of the crystal adds about 1 k. Altogether, one obtains from these reductions of entropy an increase of  $\sigma_e$  equal to  $8kT/18 \text{ \AA}^2 \approx 245$  erg/cm<sup>2</sup>. This value is about three times as large as that for the folded-chain crystal. That means a height three times as large and a free enthalpy excess three times as large as those of the critical nucleus. Hence, the probability for formation of such a fringed-micelle nucleus with an aspect ratio of about 20 is negligibly small if compared with that of a folded-chain crystal nucleus.

The *extended-chain* crystal has at its end faces free chain ends and chain folds. Hence, it is a poorly defined mixture of a fringed-micelle and a folded-chain crystal. One expects a similar mixture of contributions of the entropy reduction and energy increase to  $\sigma_e$  which would yield a value between the two extremes, 245 erg/cm<sup>2</sup> for the fringed-micelle and 75 erg/cm<sup>2</sup> for the folded-chain crystal.

Another effect playing a role in nucleation and crystal growth is the viscous resistance of the liquid against any translation and shape change of the molecule which is to be included into the crystal lattice. This adds a factor proportional to the exponential function of the activation energy for the viscous flow  $U_n$  divided by the temperature excess over the temperature  $T_2$  of the glass transition (which is about 50°C below the actually observed  $T_g$  of the liquid phase). One, hence, obtains for the nucleation rate, i.e. for the number of nuclei formed per sec and per cm<sup>3</sup>

$$I = B \exp[-U_n/k(T - T_2)] \exp(-\Delta g^*/kT) \quad (7)$$

The pre-exponential factor  $B$  contains the influence of the concentration, i.e.  $\rho_l$  for the melt and a smaller value for solution, of the number of elementary

jumps in viscous flow, of the surface to volume ratio of nuclei, and of the number of attempts per second of molecular segments to be transferred from one phase to the other one. It is rather difficult to check the dependence on these parameters on the basis of available experimental data.

Much more important is the exponential expression describing the temperature dependence of the nucleation. In the case of PE melt crystallized from tiny droplets<sup>5</sup> in the temperature range between 87 and 89°C one obtains a straight line in a plot of  $\ln I$  versus  $T$  or of  $\ln I + U_n/k(T - T_2)$  versus  $(T + T_m)^2/T^3\Delta H_f(\Delta T)$ .<sup>2</sup> In a temperature range of less than 2° the nucleation rate changes by a factor of 100. The slope yields  $\sigma^2\sigma_e = 17,500 \text{ erg}^3/\text{cm}^6$  if one assumes  $\Delta H_f = 2.9 \times 10^9 \text{ erg/g}$ ,  $T_m = 417.8 \text{ K}$ ,  $T_2 = 201 \text{ K}$ ,  $U_n = 6.3 \times 10^{10} \text{ erg/mol}$ , uses in  $\Delta g^*_f$  the factor 30.2 instead of 32, and takes into consideration the temperature influence on the surface free enthalpy (not explicitly mentioned in this short survey). Note that  $U_n$  is by about a factor of between 2 and 3 smaller than the usual activation energy for viscous flow.

From the relatively high values of  $\sigma^2\sigma_e$  one obtains  $\sigma_e = 93 \text{ erg/cm}^2$  if one assumes  $\sigma = 13.7 \text{ erg/cm}^2$  as derived from crystal growth data. The difference between  $\sigma$  and  $\sigma_e$  is the consequence of the free enthalpy excess of folds which hence turns out to be  $4.18 \text{ kcal/mol} = 17,500 \text{ J/mol}$ . This corresponds to the excess enthalpy of about eight fully relaxed gauche conformations per fold. One needs a slightly smaller number if some bond angle and length distortion is required in order to make the fold width and height fit exactly the lattice arrangement of the crystallized chain sections. This additional free enthalpy requirement of the folds is to some extent distributed over the adjacent crystal lattice which shows a distorted unit cell. This was concluded from the average volume increase of the unit cell of single crystal lamellae which is roughly proportional to the inverse thickness of lamella.<sup>8</sup>

A very small modification of the parameters and a proper consideration of the surface free enthalpy changes with temperature makes the pre-exponential factor  $B$  decrease from  $10^{47}$ , as found in the above-mentioned plotting, to  $10^{34}$  which agrees perfectly with the theoretical predictions. With a similar ease one can also modify the product  $\sigma^2\sigma_e$ . Hence, one must not pay too much attention to the exact values of the parameters deduced from nucleation experiments in a relatively narrow temperature range. What matters more is the possibility of a quantitative description of the nucleation phenomena, in particular the enormous variation with temperature.

The existence of two factors with a different temperature dependence in the expression for the nucleation rate, Eq. (7), yields an increase of the rate at a small supercooling up to a maximum and a subsequent drop with approach to the glass transition temperature of the liquid phase. The variation with the temperature as calculated for PE and poly(chlorotrifluoroethylene) (PCTFE) is shown in Figure 2.



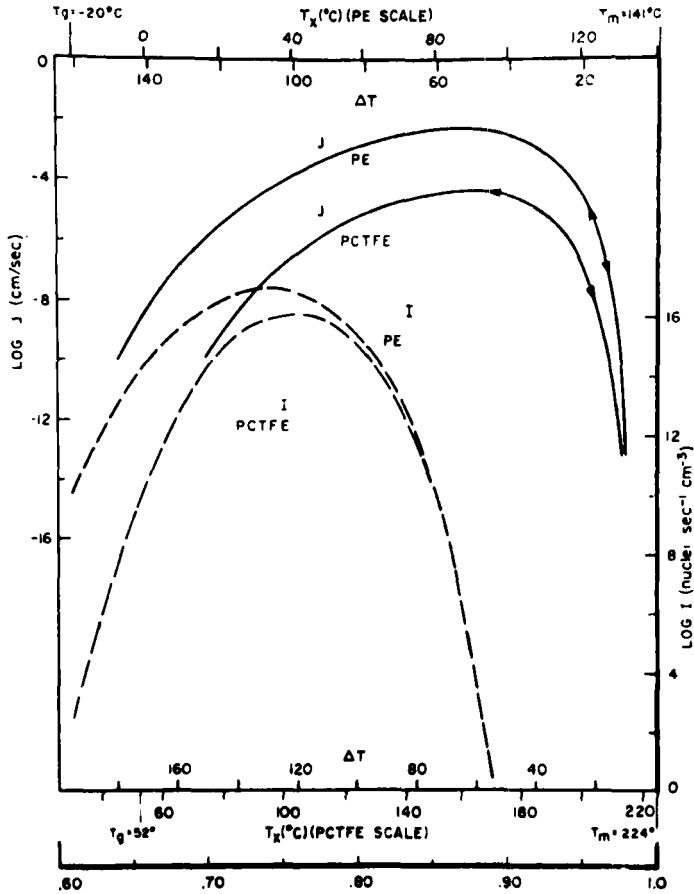


FIGURE 2 Nucleation,  $I$ , and crystal growth,  $J$ , rates of polyethylene and poly(chlorotrifluoroethylene) as a function of temperature,  $T$ , or supercooling,  $\Delta T$ , according to Hoffman and Weeks.<sup>3</sup> Reprinted with permission of the American Institute of Physics.

At the critical dimensions of the homogeneous primary nucleus the rate of the nucleation is zero because such a nucleus can lose equally well the excess enthalpy by moving to smaller or to larger dimensions. It is only at an excess  $a > a^*$  and  $c > c^*$  that the lateral growth prevails over the lateral dissolution. The growth of the nucleus is guaranteed as soon as the critical dimensions are surpassed.

In this consideration one can completely neglect the growth of  $c$  beyond  $c^*$  which requires complicated axial displacement of the chains in the crystal lattice. This motion is rather difficult not only because the lattice forces oppose such an axial displacement but more importantly because an increase of

crystal thickness can only be achieved by a simultaneous displacement of all the rest of the linear macromolecule involved. As a consequence of folding, one half of the stems has to move in the opposite direction to the other half. Such a complicated cooperative motion demands so much higher driving forces than the lateral deposition of new chain sections that its contribution to the growth of the primary nucleus can be completely disregarded.

## GROWTH OF CRYSTALS

The growth of the crystals depends on the rate of the molecular deposition on the lateral faces of the nucleus. No growth occurs in the chain direction because the folds there interrupt the crystal lattice and block, by their fixation in the crystal, any simple mechanism of thickness increase.

The lateral deposition of new straight chain sections can be best described in terms of a secondary and a tertiary nucleation. The former one applies to the deposition of the first straight section on a smooth flat surface which starts a new layer of chains with a thickness  $b_0$  and the latter one to the addition of such sections on the outer ledges of the secondary nucleus up to the completion of this layer. Since the nuclei are formed on a pre-existing body of the same lattice structure one can consider both cases as a primary and secondary heterogeneous nucleation. The corresponding values of  $\Delta g_f$  and  $c^*$  will be designated by subscripts 1 and 2, respectively.

In both cases one has to do with a substantially smaller increase of the free enthalpy than in the primary homogeneous nucleation case. For the deposition of the first stem one has

$$\Delta g_{f1} = -\rho_c a_0 b_0 c \Delta G_f + 2b_0 c \sigma + 2a_0 b_0 \sigma_e \quad (8)$$

while for any next stem the increase of the free enthalpy turns out to be

$$\Delta g_{f2} = -\rho_c a_0 b_0 c \Delta G_f + 2a_0 b_0 \sigma_e \quad (9)$$

Here,  $a_0$  is the width of the chain parallel to the growth face and  $a_0 b_0$  is its cross-section. The free enthalpy requirement for the chain deposition on the ledge formed by the previously deposited chains of the layer equals zero for

$$c^*_2 = 2\sigma_e / \rho_c \Delta G_f \quad (10)$$

which is just half of the critical height  $c^*$  of the homogeneous primary nucleus. Any value  $c$  larger than  $c^*_2$  yields a negative  $\Delta g_{f2}$ . Hence, in such a case the growth of the crystal up to the completion of the monomolecular layer is a very fast process. The time-consuming step is only the deposition of the first stem with a free enthalpy requirement

$$\Delta g_{f1} = 2b_0 c \sigma + \Delta g_{f2} = 2b_0 [(c - c^*_2) (\sigma - a_0 \sigma_e / c^*_2) + c^*_2 \sigma] \quad (11)$$

which increases with  $c$  while  $\Delta g_{f2}$  decreases with  $c$ . The higher the added monomolecular layer the more difficult is the deposition of the first stem while that of new stems on the ledge formed by the deposited stems is highly enhanced. The proper consideration of both effects yields the growth rate of the crystal and the average height, i.e. the lamella thickness  $L$  which turns out to be larger than  $c^*_2$  by a term  $\delta l$ .

The so-called lamella thickness  $L$  shows a very peculiar singularity at  $\Delta G_f = 2\sigma/a_0$ . In the case of PE with  $\sigma/a_0 = 3 \times 10^8$  erg/cm<sup>3</sup>, this happens at a supercooling  $\Delta T = 103.1$  K, i.e. at  $T = 314.7$  K or 41.5°C. This is a very substantial supercooling which has never experimentally been investigated. But there is also no indication of an approach to such a singularity with smaller supercooling so that such a catastrophe seems to be very improbable. It is most likely a consequence of some improper assumption of the crystallization mechanism. Indeed, by considering the possibility that a fraction  $\psi$  of the free enthalpy of fusion is apportioned to the activation of the molecular fixation on the crystal and the remainder  $1-\psi$  to the rejection, Lauritzen and Hoffman<sup>9</sup> were able to eliminate this singularity. They obtained for the linear rate of crystallization

$$J = N_0 P(kT/h) \exp(2a_0 b_0 \sigma_e \psi / kT) \exp(-4b_0 \sigma \sigma_e / kT \rho_c \Delta G_f) \quad (12)$$

where

$$P = (kT/b_0 c_0) \{1/(2\sigma - \psi a_0 \rho_c \Delta G_f) - 1/[2\sigma - (1 - \psi) a_0 \rho_c \Delta G_f]\}$$

and for the average lamella thickness

$$L = 2\sigma_e \Delta G_f + (kT/2b_0 \sigma) [2 + (1 - 2\psi) a_0 \rho_c \Delta G_f / 2\sigma] / \{(1 - a_0 \rho_c \Delta G_f \psi / 2\sigma) \times [1 + a_0 \rho_c \Delta G_f (1 - \psi) / 2\sigma]\} \quad (13)$$

Here,  $N_0$  is the number of sites per unit length of the growth face of lamella available for the deposition of the first straight stem which initiates the heterogeneous surface nucleation. In order to simplify the presentation the viscosity factor is purposely omitted in Eq. (12).

The influence of the choice of  $\psi$  is shown in Figure 3 for parameter values of  $T_m = 500$  K,  $\sigma = 10$  erg/cm<sup>2</sup>,  $\sigma_e = 100$  erg/cm<sup>2</sup>,  $a_0 = b_0 = 5$  Å,  $\Delta H_f = 3 \times 10^9$  erg/g,  $U_n/N_A k = 700$  K ( $N_A$  is the Avogadro number), and  $J_0 = 10^{10}$  cm s<sup>-1</sup> which are close to, but not identical with, those of linear PE. The value  $U_n$  is (as already mentioned) too small by a factor between 2 and 3 and that of  $J_0$  is most likely too large by a factor of  $10^4$ . One sees very clearly how the decrease of  $\psi$ , i.e. of the deposition probability, moves the temperature of thickness singularity to lower temperatures but does not remove it completely up to  $\psi = 0$ .

A small  $\psi$  also seems to be better adjusted to polymeric systems as, for instance, linear PE and isotactic polystyrene.<sup>9</sup>

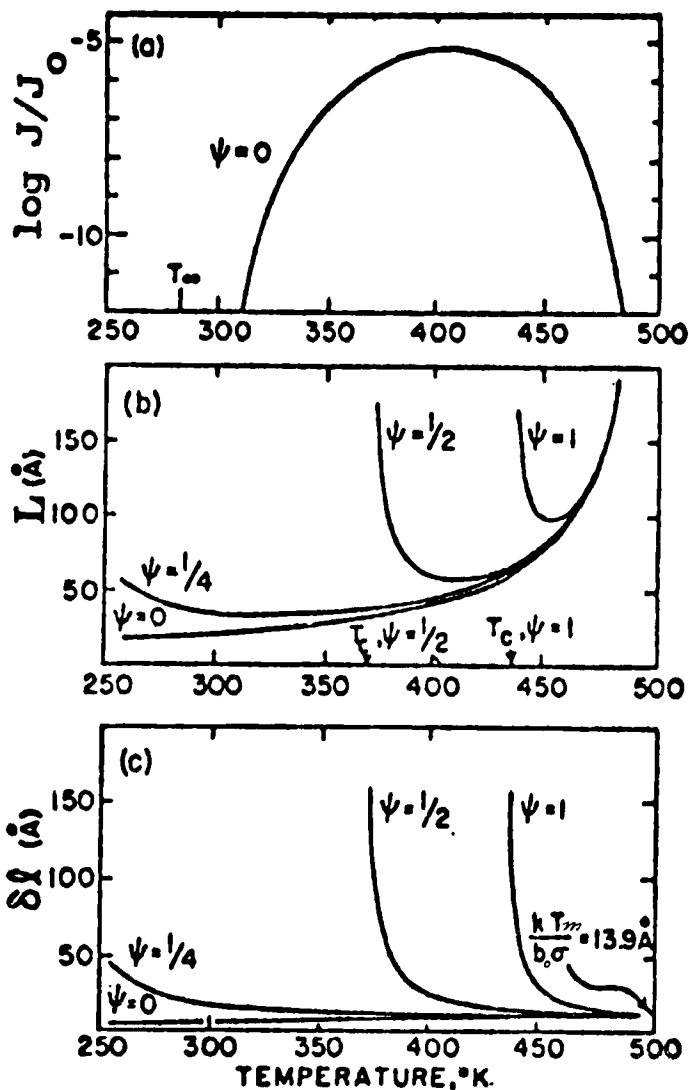


FIGURE 3 Linear growth rate  $J$ , lamella thickness  $L$ , and  $L - c^*_2 = \delta l$  as functions of temperature for several values of the deposition factor  $\psi$ . The parameters used in the calculation are:  $T_m = 500$  K,  $T_2 = 280$  K,  $\Delta H_f = 3 \times 10^9$  erg/cm<sup>3</sup>,  $\sigma = 10$  erg/cm<sup>2</sup>,  $\sigma_e = 100$  erg/cm<sup>2</sup>,  $a_0 = b_0 = 5$  Å,  $U\eta/N_A k = 700$  K,  $J_0 = 10^{10}$  cm/s. After Hoffman *et al.*<sup>2</sup>

The molecular weight dependence enters the theoretical expressions by a modification of the heat of fusion and of the entropy of the amorphous and crystalline component caused by the finite length of the chain and the difference between the mers in the chain and the end-groups. These effects will not be

considered here explicitly because they are not very conspicuous if one treats real polymers with at least many hundreds or even thousands of repeat units. But they become very important with the oligomers if the chain length is of the same order of magnitude or even smaller than  $L$ . Such molecules, e.g. paraffins in the case of PE, cannot form folded-chain crystals if their length is not substantially larger than  $L$ . In the case of the very monodisperse poly (ethylene oxide) samples,<sup>10</sup> one has shown that at any crystallization temperature the lamellae have not the thickness  $L(T)$  but the closest smaller or equal one which is an integral fraction of chain length  $l$ , i.e.  $l$ ,  $l/2$ ,  $l/3$ ,  $l/4$ . This very clearly demonstrates the tendency of exclusion of the chain ends from the crystal lattice and their accommodation as cilia on the fold-containing surface of lamella. Such an effect is proportional to  $1/M$  and, hence, hardly matters at very high  $M$  although it is of prevailing importance with the oligomers.

Under a high pressure, 3,000 atm (about 3 GPa) and higher, PE tends to crystallize in what is termed extended-chain crystals with a thickness of many thousand Å in the chain direction.<sup>11</sup> In extreme cases one has extended a large fraction of the crystallized chains although a substantial fraction still has to fold back in order to be accommodated even in the thickest crystals. It turns out that at the high temperatures, about 200°C and higher, and the high pressures of crystallization, a hexagonal, quasinematic phase is formed with an extremely low  $\Delta H_f$ . This yields a very high  $L(T)$ , about 1,000 Å, which during a prolonged storage at the high crystallization temperature and pressure increases much more rapidly than in the case of orthorhombic PE although the relative increase  $\Delta L/L\Delta t$  is smaller.<sup>12</sup>

The present state of the kinetic theory of crystallization from the fully relaxed melt or solution at rest seems to be very satisfactory.<sup>2,13</sup> The theory yields the correct temperature and molecular weight dependence of the average thickness of folded-chain lamellae, of the nucleation and growth rate with a maximum at modest and subsequent drop at larger supercooling, and sufficiently well avoids the pitfall of thickness catastrophe at a relatively small supercooling which plagued all former formulations. But it still has some problems with the fractionation, the amorphous surface layers, and the long period changes during the plastic deformation by drawing or rolling (compression).

In the crystallization from a dilute solution, the higher molecular weight components are predominantly in the crystals and the lower molecular weight components are enriched in the remaining solution.<sup>1</sup> The explanation would be simple if the rejected molecules were shorter than  $L$  and the crystallized molecules longer than  $L$ . But the separation is at about four or five times the lamellar thickness. This seems reasonable if instead of individual chain segments of the length  $L$ , one would have bundles of four or five such chain segments which are included as an entity to the growing crystal. Such pre-

bundling in the melt or solution would, hence, exclude from the crystallization all those chains which are too short for the formation of the bundle.

This idea was quantitatively treated by Allegra,<sup>14</sup> who, from statistical and energy considerations, indeed found that in an infinitely long chain, bundles of at least three chain sections can be formed with an average loop length agreeing well with the lamella thickness of the crystals growing at the same temperature. If the molecule is not long enough for the formation of such a bundle, it has a much reduced chance for crystallization. The loop length is a consequence of the dynamic equilibrium between the energy of binding of short, parallel chain sections into a quasicrystalline lattice (subcritical nucleus) and the Brownian motion of the large loops. This length either determines the actually observed lamella thickness or agrees so well with the kinetically derived value that the loops can be accepted by the growing crystal without any dimensional modifications.

In normal solutions this concept does not disagree with data from light scattering, intrinsic viscosity, or translational diffusion which have always been successfully interpreted in terms of randomly coiled macromolecules without any internal binding of rather distant sections. The solutions are all so much above the crystallization temperature of the polymer even in the case of theta solutions that, according to Allegra, no bundles are yet formed. The situation is a little more precarious in supercooled melts and still more in melts solidified in the amorphous state where the small angle neutron scattering has revealed the same type of macromolecular coiling as in theta solutions. Since one is below the melting temperature one would expect, according to Allegra, the existence of bundles with a gyration radius and angular dependence of small angle neutron scattering different from those obtained from dilute theta solutions where the bundling does not yet occur.

If the bundling is limited to the immediate vicinity of the growing crystal, it would not contribute significantly to the scattering of the bulk but would aid the crystallization. This would certainly make all those people happy who have difficulties with the high rate of chain inclusion into the growing crystals in spite of the fact that it requires the pulling of chains out of the melt or solution.

Amorphous surface layers certainly exist in the crystals obtained from the melt and in the annealed crystals obtained from the solution. Their thickness and density defect was derived from the density, the small angle X-ray scattering, the NMR absorption of crystals in contact with a swelling liquid, and from the fuming nitric acid etching.<sup>15</sup> The surface layers contain more material than one would expect from the model of regular folds with adjacent re-entry and from the cilia, i.e. from the free ends of molecules which cannot be incorporated into the crystal lattice.

In the low molecular weight samples the crystals from the solution are practically free of such layers, as can be concluded from their high density which

is almost equal to that of the ideal crystal lattice and from the observation of dislocation loops on two superimposed single crystals with matching lattice orientation which makes the conventional Moiré pattern disappear.<sup>16</sup> Such a matching is only possible if the information about the lattice orientation is transmitted from one lamella to the other one through the boundary. Hence, the boundary must be composed of sufficiently regular loops reflecting the lattice order. Any coherent amorphous layer completely separating the two crystal lattices would make such a transmission of orientation impossible.

The thickness of the amorphous surface layers seems to depend uniquely on the highest temperature the lamella was ever exposed to. It was attempted to be explained by a fraction of loops with random re-entry (switch-board arrangement of some loops)<sup>17</sup> and by the assumption of so intense surface adsorption of uncrystallized very long macromolecules that they cannot be washed away by the solvent.<sup>2</sup> According to a thermodynamic or statistical dynamic analysis, the loops with adjacent re-entry cannot be made so loose that they would yield the actually observed thickness of the amorphous surface layers. The explanation by adsorbed molecules cannot explain the changes of surface thickness with the temperature of annealing and its independence of the duration of annealing when the long period and the density steadily increase while the fraction of the amorphous component decreases.

The kinetic theory of polymer crystallization assumes perfect crystalline order inside the lamella with the thickness  $L$  and considers the fold only in terms of the excess surface free enthalpy  $\sigma_e - \sigma > 0$ . Hence, it cannot handle any amorphous surface layer. Its assumptions and conclusions seem to be well in agreement with the single crystals obtained from the dilute solutions of relatively low molecular weight samples which are almost ideal without any significant amorphous surface layer. In all other cases one remains within the theoretical model if one assumes that the amorphous surface layers are a secondary effect occurring after crystallization, e.g. by adsorption of long molecules on the surface containing the regular folds with adjacent re-entry.

The reduction of the long period during plastic deformation, i.e., by drawing or rolling<sup>18-20</sup> which transforms the lamellar into fibrous structure, is completely unexplainable by the kinetic theory of crystallization. The reduction takes place if the starting material has a high  $L$  and the plastic deformation is performed at a low temperature. It turns out that the long period ( $L_d$ ) obtained is primarily a function of the actual temperature ( $T_d$ ) in the destruction zone where the lamellar structure is transformed into the fibrous structure.<sup>21</sup> It is practically independent of that of the starting material and very nearly identical to that ( $L_c$ ) that one obtains if one crystallizes the material from a fully relaxed melt at the same temperature  $T_d$  (PE,<sup>22</sup> isotactic polypropylene,<sup>23</sup> Nylon 6<sup>24</sup>). This would suggest an explanation in terms of melting the lamellae of the original material and recrystallization of the melt into the folded-chain blocks

of the newly-formed fibrous structure. An analysis of the work for plastic deformation,<sup>25</sup> however, shows that in spite of a substantial local increase of temperature one has not enough energy available for raising the temperature to the melting point and still less for the heat of fusion needed for the subsequent melting. Hence, one has to conclude that the shearing displacement of the chain stems in the plastically deformed lamellae so much enhances the axial chain mobility that the crystal is able to assume the energetically most favorable shape. According to the thermodynamic theory of free enthalpy of polymer crystals,<sup>26</sup> this state is achieved at a certain length  $L_{TD}$  which for any polymer depends uniquely on the temperature, the axial and rotational chain mobility, and the surface free enthalpy. In the case of linear PE, this value very much agrees with  $L$  obtained from the kinetic theory of crystallization from the melt at the same temperature, i.e. at the supercooling  $\Delta T = T_m - T$ . Drawing experiments on other systems as, for instance, isotactic polystyrene where the long period is very little dependent on temperature, would be highly welcome. On the other hand, one needs a theoretical calculation of thermodynamic stability for any polymer system of interest because one presently has only a rough theory for the linear PE.

### CRYSTALLIZATION FROM A STRAINED LIQUID<sup>27</sup>

As soon as the liquid phase contains partially oriented and extended chains, the phase transition from the liquid to the crystal is very much modified because the enthalpy and entropy of the liquid phase differ from the values they have in a fully relaxed liquid. The enthalpy decreases by  $\delta H_{a\epsilon}$  as a consequence of the better packing, which reduces the distance between adjacent chains, and of the chain extension, which increases the fraction of the lower energy trans conformations. The entropy decreases by  $\delta S_{a\epsilon}$  as a consequence of the reduction of available conformations with the chain extension and orientation ( $\delta S_{a\epsilon 0}$ ) and as a consequence of the reversible enthalpy reduction ( $\delta H_{a\epsilon}/T$ ).

Even in the case of no change of the enthalpy, i.e. no change of the distribution between gauche and trans conformations and of the chain packing, the orientation of chains reduces the entropy of the liquid phase and, hence, increases the equilibrium melting temperature  $T_{m\epsilon}$  above  $T_m$  of the fully relaxed melt. A concurrent decrease of the heat content,  $\delta H_{a\epsilon}$ , of the partially oriented and better packed liquid would of itself reduce this increase of  $T_{m\epsilon}$ . But it reduces also the entropy of the liquid phase by  $\delta H_{a\epsilon}/T$  which more than compensates for the effect of  $\delta H_{a\epsilon}$  on melting or crystallization temperature because  $T$  is always smaller than  $T_{m\epsilon}$  or  $T_m$ . Hence, it never depresses the melting point below the ideal value of the fully relaxed system at rest.



A strain applied to the melt at any temperature increases the free enthalpy of the melt,  $G_a(T) - G_{ae}(T) < 0$ , and hence yields  $\delta H_{ae} - T\delta S_{ae} < 0$ . From this one derives the equilibrium melting or crystallization temperature

$$T_m = \frac{\Delta H - \delta H_{ae}}{\Delta S - \delta S_{ae}} = T_m \frac{1 - \delta H_{ae}/\Delta H}{1 - T_m \delta S_{ae}/\Delta H} = T_m \frac{1 - \delta H_{ae}/\Delta H}{1 - (T_m/T)\delta H_{ae}/\Delta H} \quad (14)$$

The equilibrium crystallization or melting temperature  $T_{m\epsilon}$  of the strained melt which determines the supercooling  $\Delta T_{m\epsilon} = T_{m\epsilon} - T$  is always higher than  $T_m$  of the unstrained melt as long as  $T < T_m$ . The increase of  $T_{m\epsilon}$  over  $T_m$  and the decrease of the enthalpy of fusion  $\Delta H_{ae}$  below  $\Delta H_f$  influence the size of the primary and secondary nuclei, the nucleation rate and growth, and the average

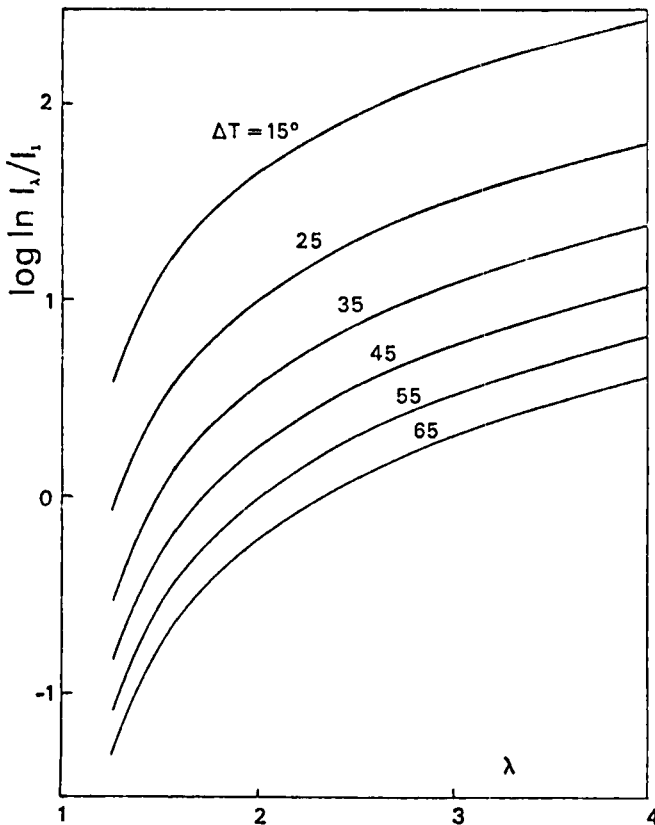


FIGURE 4 Log  $\ln$  of relative nucleation rate,  $I_\lambda/I_1$ , of primary nuclei as a function of extension ratio,  $\lambda$ , for various supercooling,  $\Delta T$ , calculated under the assumption that:  $T_m = 312.2$  K,  $\Delta H_f = 70.3$  J/g,  $\rho = 1.18$  g/cm<sup>3</sup>,  $E = 7.08$  MPa at 90°C as determined from C of the Mooney equation,  $\sigma = 8.5$  erg/cm<sup>2</sup>, and  $\sigma_e = 35.3$  erg/cm<sup>2</sup> (slightly cross-linked trans-polyisoprene<sup>32</sup>).

thickness of lamellae. These changes can be quite spectacular in all the effects depending exponentially on the free enthalpy of fusion, i.e. in the growth and nucleation rate which can increase by many decades (Figure 4). The oldest example is the crystallization of strained rubber. The technically most important example is the crystallization in the jet during spinning. About ten years ago one has discovered the crystallization in stirred solution.

Moreover, the morphology of the crystal phase obtained from a strained liquid phase is completely different from that obtained from a fully released liquid. Instead of spherulites growing almost isotropically in all directions from randomly oriented primary nuclei one observed an extremely anisotropic growth pattern originating from linear primary nuclei (row nuclei). Highly oriented cylindrites or spherulites compressed in the strain direction and having their primary nuclei more or less aligned in rows parallel to the strain are formed from the strained melt. Long fiber-like shish-kebab structures develop from the strained dilute solution. In both cases, one has central row nuclei epitaxially overgrown by folded-chain lamellae which are either densely packed (cylindrites) or irregularly spaced (shish-kebab). The lamellae are helically twisted at a small strain and almost planar at a high strain. In the case of a very large spacing of nuclei, anisometric spherulites can develop with their short axis in the strain direction.

Such a crystallization is of a great technical importance because it occurs in practically all industrial molding and extruding operations where the solidification takes place from the more or less strained melt or solution, i.e. not only in fiber spinning and in film blowing, extrusion, and hot rolling, but also in the molding of bulkier objects. On the other hand, one expects to obtain extremely strong fibers from the highly crystalline filaments formed in a stirred solution. One, hence, understands the technical interest in the crystallization from a strained solution and melt because a better theoretical grasp of the effect would permit an improvement of existing technical methods and eventually yield new material with better mechanical properties than is presently available.

## STRAINED NETWORK<sup>27</sup>

If one strains a network the deformation of chains and their average orientation remain constant in time as a consequence of the fact that the cross-links are permanent and, hence, do not allow any large-scale rearrangement of the network structure. In the simplest approach, one applies the microscopic deformation to the system of cross-links and lets the connecting chains relax completely. This is certainly not correct because the forces on each cross-link depend not only on the bulk deformation but also on the location and displace-

ment of all the cross-links connected by chain segments with the cross-link under consideration and by the contour and end-to-end length of these segments. A realistic description of the network deformation on this basis is so complicated that it has not yet been performed in a satisfactory manner. The deficiencies of the above-mentioned, so much simpler, conventional treatment, which displaces the cross-links in the same manner as the bulk deformation displaces the points of a continuum, are best characterized by the statement of Dušek and Prins<sup>28</sup> that no cross-linked system exists which in its mechanical properties would agree completely with the theoretical predictions.

The oldest example of the crystallization from a strained amorphous phase is that of natural rubber under uniaxial tension.<sup>29</sup> As a rule, the crystallinity obtained is very small, in the vicinity of 10%. The crystallization and associated effects were amply studied with natural rubber and other elastomers as, for instance, trans-isoprene, chloroprene, transpentaener, and isotactic polystyrene.

At room temperature the crystallization rate of the unstrained natural rubber is imperceptibly small although one is far below the melting point. But strained to  $\lambda$  about 3 it crystallizes very rapidly. Concurrently, the Avrami exponent  $n$  drops from 3 of the unstrained rubber to 1 or even below for the biaxially strained sample.<sup>30</sup> Such an effect can be interpreted as a conversion from the initial three-dimensional to the one-dimensional growth with some restrictions which may come from the cross-links. The morphology of crystallization depends markedly on the applied strain. At a small strain one obtains folded-chain lamellae which are more or less perpendicular to the strain direction. They seem to grow epitaxially on the linear row nuclei which form first. At a high strain the structure is fibrillar with the microfibrils parallel to the strain.<sup>31,32</sup>

As shown by Hay *et al.*,<sup>33</sup> the formation and prevalent linear growth of nuclei in the strain direction in strained elastomers can be well explained on the basis of the nucleation theory just outlined. If by any mechanism a crystalline nucleus is formed in the strained amorphous matrix (homogeneous nucleus) or there is a foreign crystalline particle (heterogeneous nucleus) present, it very much distorts the stress field because its elastic modulus is so much higher, by a factor of a few hundred, than that of the not yet crystallized supercooled melt in which it is embedded. At points on the stress axis (poles), the stress is higher than average. The ratio of the stress on the poles to the bulk stress is about 2 for very rigid spheres in a soft medium. At points on the equator the stress is lower than average. The stress concentration at the poles enhances the nucleation rate, possibly resulting in a formation of another nucleus. Such nuclei alignment parallel to the stress will cause an even greater stress concentration at the poles and the formation of further aligned nuclei. Consequently, if the rate enhancement is sufficiently large at the poles of the nucleus, it will prefer-

entially grow into a fibrillar structure parallel to the strain or stress direction. For a perfect rubber one can neglect the changes in heat content,  $\delta H_{a\epsilon} = 0$ . The change in entropy is

$$\delta S_{a\epsilon 0} = k\nu(\lambda^2 + 2/\lambda - 3)/2 \quad (15)$$

where  $\nu$  is the number of load bearing chains per  $\text{cm}^3$ ,  $\lambda = 1 + \epsilon$  is the elongation ratio, and  $\epsilon$  is the strain. If one uses the experimental data for natural rubber,<sup>34</sup>  $\Delta H_f = 70.3 \text{ J/g}$ ,  $T_m = 312.2 \text{ K}$ ,  $\sigma = 8.5 \text{ erg/cm}^2$ , one obtains, as shown in Figure 5 as a function of extension ratio, the relative nucleation rates  $I_a/I_p$  for the first adjoining nucleus at the stress poles of the primary nucleus which, as a doublet, starts the row nucleation ( $I_a$ ) as compared with that of the primary nucleation ( $I_p$ ). For the sake of simplicity, the authors assumed that the primary nucleus is spherical.

The nucleation of doublets has to compete with the formation of primary nuclei which may happen any place in the whole volume while the active volume for the enhanced rate of row nucleation,  $I_a$ , is only the immediate vicinity of the stress poles of the primary nucleus. Since this volume is of the same order of magnitude as the volume of the nucleus, i.e. about  $10^5 \text{ \AA}^3$ , the ratio  $I_a/I_p$  has to be about  $10^{19}$  in order to have equal probability of more or less isotropic primary nucleation and row nucleation initiation by doublet formation.

For  $25^\circ\text{C}$  supercooling and  $\lambda = 2$ , the ratio of the rates  $I_a/I_p$  is  $10^{18}$ . At a very high supercooling ( $65^\circ\text{C}$ ), this ratio is only of the order of  $10^2$  to  $10^4$ , and, hence, one might expect the primary nucleation to dominate. At a low supercooling ( $15^\circ\text{C}$ ), however, the ratio can go as high as  $10^{100}$  so that from rate consideration every primary nucleus will develop into a fibril.

This thermodynamic analysis is applicable to strained network, melt, and solution. It demonstrates very well how much the local depression of the entropy of the liquid phase enhances the growth of the linear nuclei. Once the linear or row nuclei are formed they carry most of the load of the stress field and, hence, let the rest of the liquid sample relax. As a consequence of such a substantial relaxation the crystallization proceeds in a more conventional manner. The row nuclei act as heterogeneous nuclei for this secondary epitaxial crystallization which yields the folded-chain lamellae perpendicular to the strain direction.

## STRAINED MELT<sup>27</sup>

With sufficiently high molecular weight, macromolecules are so entangled that the resulting network dominates the bulk flow properties, e.g. the viscosity which turns out to be proportional to  $M^{3.4}$ . But the cross-links formed by entanglements are not permanent. They are destroyed and reformed under the

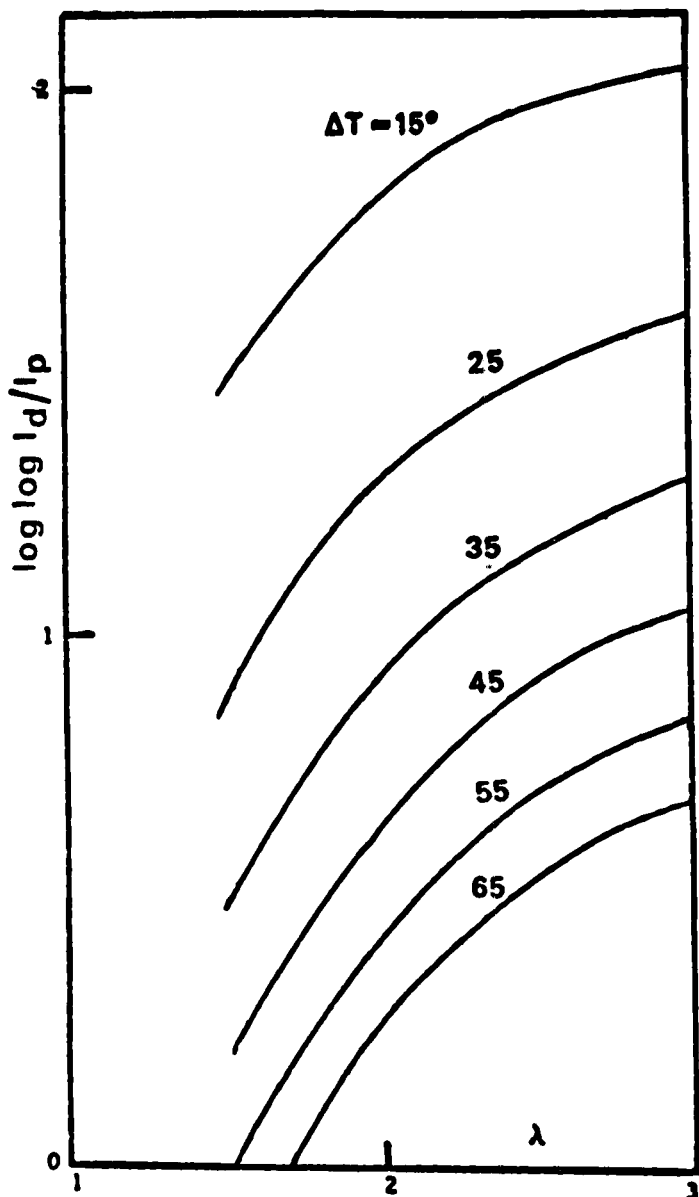


FIGURE 5  $\ln$  of the relative nucleation rates of doublets and primary nuclei,  $I_d/I_p$ , versus extension ratio,  $\lambda$ , for various supercooling,  $\Delta T$ , as calculated by Hay *et al.*<sup>33</sup> for slightly cross-linked trans-polyisoprene.<sup>32</sup>

influence of the Brownian motion and the applied stress field. A permanent chain orientation and extension is only possible in a constant flow field with a transverse and/or longitudinal gradient which exposes the melt to a constant stress field. The application of any finite fixed deformation induces a flow which in a relatively short time makes the liquid relax completely so that any initial orientation and stretching effect disappears with time.

The chain extension and orientation can be maintained by a flow with a velocity gradient  $\dot{\gamma}$  parallel (longitudinal) or perpendicular (transverse) to the flow direction. In the former case one has a jet flow with a steadily decreasing or increasing cross-section corresponding to the increasing or decreasing flow velocity, respectively. In the latter case of a capillary or Couette flow, the cross-section of each flow line remains constant. Fiber spinning and film extrusion are the most common cases of axial and planar jet flow, respectively, which play an important role in polymer technology. The purely compressional acoustic wave represents a periodic longitudinal gradient. As a rule, the longitudinal gradient is very small. A particularly large longitudinal gradient up to  $10^3 \text{ s}^{-1}$  is obtainable with head-on impingement of two anti-parallel jets.<sup>35</sup>

The steady-state orientation and extension in the flow with a longitudinal or transverse gradient depends on the dimensionless gradient parameter  $\beta$

$$\beta = M[\eta]\eta_s\dot{\gamma}/N_AkT \quad (16)$$

defined for infinitely dilute solutions. Here,  $[\eta]$  is the gradient-dependent intrinsic viscosity in a flow with the transverse gradient  $\dot{\gamma}$ ,  $M$  is the molecular weight of the solute, and  $\eta_s$  is the shear viscosity of the solvent. For a more concentrated solution,  $[\eta]\eta_s$  has to be replaced by  $(\eta - \eta_s)/c$  where  $\eta$  is the viscosity of solution. Since in the melt and concentrated solution  $\eta \gg \eta_s$  one can write

$$\beta = M\tau/N_AkTc \quad (16a)$$

with the stress  $\tau = \eta\dot{\gamma}$  and concentration  $c$ . The parameter  $\beta$  depends strongly on  $M$  because for not too low molecular weight melts one has  $\eta(M) \sim M^{3.4}$  so that  $\beta$  is proportional to  $M^{4.4}$ . Even in dilute solutions according to Eq. (16),  $\beta$  is proportional to between  $M^{1.5}$  and  $M^2$ . The high dependence on  $M$  means that the high molecular weight tail of the molecular weight distribution of the polymer will be most affected by the flow and, hence, will crystallize first. Such a fractionation effect was reported very often in the crystallization from a stirred polymer solution.

At any  $\beta$  value, the coil deformation is much larger in the flow with a longitudinal than in the flow with a transverse gradient. In the former case, the coil is fully extended at  $\beta_l = 0.5$  while in the latter case this happens at  $\beta_{tr} \sim M^{1/2}$ . But the smallness of the longitudinal gradient in conventional equipment makes it much more difficult to reach even the relatively small critical value 0.5 of  $\beta_l$ .

Hence, in most cases, the actual coil deformation and orientation is very small although the extension ratio in extrusion and spinning as measured by the reduction of the material cross-section can be as high as 100. The situation, however, is much more favorable in the case of two impinging jets.

On the other hand, the constant flow pattern, i.e. the same gradient, has to be applied to each volume element of the liquid for a sufficiently long time,  $t > t_{\text{rel}}$ , so that the molecule can indeed assume the steady-state conformation corresponding to this gradient. The relaxation time  $t_{\text{rel}}$  is roughly equal to  $\beta/\dot{\gamma} = M\eta/N_A kTc$  (melt and concentrated solutions) or  $M[\eta]\eta_s/N_A kT$  (dilute solutions) so that an increase of the deforming stress  $\beta$  by higher  $\eta$  or  $M$  is completely counterbalanced by the longer time needed for achieving the steady-state conformation.

If this is not the case one has to deal with molecules in a transient state between the completely randomized shape in the liquid at rest and the limiting steady-state deformation in the flow. This hardly matters in the conventional flow with a transverse gradient where the volume element can be exposed to the same flow pattern as long as one wishes. But it is dominant in the flow with a large longitudinal gradient which, as a rule, cannot be applied to the volume element for so long a time that the molecule, in spite of the finite relaxation time for conformational changes, could assume the limiting shape required by the gradient. As a consequence in such a flow, the macromolecule extends and orients less than calculated for the steady state.<sup>36,37</sup>

The best demonstration of the transient effects was performed in the impinging jet instrument which yields extremely high longitudinal gradients, up to  $10^3 \text{ s}^{-1}$ . If the flow in the jets is negative, one has a positive longitudinal gradient in the axis of the jets, i.e. a gradient with the same direction as the velocity, and a negative gradient in the perpendicular direction in the symmetry plane of the instrument. The flow is rather homogeneous as far as the gradient is concerned. It can be written as

$$\vec{v} = \dot{\gamma}_i(-x/2, -y/2, z) \quad (17)$$

if  $z$  is the axis of the jets and the  $xy$  plane with  $z = 0$  is the symmetry plane of the instrument.

In spite of the homogeneous nature of the flow field with practically the same gradient in a wide area, one obtains the fibrillar crystallization only in the jet axis and practically none outside of it. Very much the same applies to the birefringence. The reason for this is the time the volume element, and with it the macromolecule, is exposed to the longitudinal gradient.<sup>38</sup> It is relatively short in all flow lines outside the symmetry axis because it is proportional to the ratio of the flow line length and velocity. In the axis, however, the velocity at the symmetry plane,  $z = 0$ , is zero so that the volume element is exposed to the same gradient  $\dot{\gamma}$  substantially longer than on any other flow line. As a

consequence of so much longer exposure, the coiled macromolecule in this volume element can better approach the equilibrium shape corresponding to the gradient than can the molecules on adjacent flow lines. It is substantially more extended and better aligned while the rest are still to a large extent in the almost randomly coiled conformation unable, in the too short time, to reach the limiting deformation requested by the gradient. Hence, its rate of crystallization is much higher than in the rest of the liquid. One obtains here an almost fully linear fiber with a relatively small fraction of chain folds.

The technically most important jet flow with longitudinal gradient is that of fiber spinning and film extrusion. The melt or solution flows first through a conical or tapered linear die with a decreasing cross-section so that the velocity of the sample steadily increases. The flow, hence, has not only a transverse gradient with maximum velocity in the axis and zero value at the walls, but also a longitudinal gradient. Both enhance chain orientation and extension although the latter one is more efficient than the former. The transverse gradient disappears in the purely jet flow after the material has left the die. The action of the remaining longitudinal gradient partially persists up to solidification yielding a combination of row-nucleated cylindrites (shish-kebab) and spherulites in the fiber as spun<sup>39</sup> or the film as extruded.<sup>40,41</sup> At slow spinning with a small longitudinal gradient, the fiber, as spun, has predominantly spherulitic structure. The morphology is gradually replaced by oriented cylindrites if one increases the uptake rate and, hence, increases the extension ratio and longitudinal gradient.

The comprehensive study of polyethylene films crystallized from a strained melt has shown that under a high strain the planes of lamellae are perpendicular to the strain. The small (SAXS) and wide (WAXS) angle X-ray scattering reflect the almost perfect lamellar and crystal lattice orientation. With a decreasing strain the density of the rows decreases and the ribbon-like lamellae start to be helically twisted.<sup>42</sup>

Some experiments have shown that the shish-kebab morphology can be obtained also in the capillary flow which has no velocity component with a longitudinal gradient.<sup>43</sup> It may be caused by another effect closely connected with the peculiar flow pattern of polymer melts and concentrated solutions. From the time dependence of viscosity of high molecular weight polymer solutions in viscous solvents, it had been suggested that by the enhanced chain entanglements the shearing first produces a network which as a rule gets broken down into loosely connected kinetic elements.<sup>44</sup> These consist of highly entangled macromolecules forming a network of almost spherical shape. The few connections between two adjacent elements are highly strained macromolecules partially entangled in both of them. They may serve as the starting point for a row nucleus and, hence, initiate the shish-kebab crystallization.



A technically important modification of the shish-kebab morphology was obtained by fiber or film extrusion and film blowing in an extremely high temperature and pressure gradient.<sup>45</sup> When the superstructure is perfected by annealing, the resulting material displays an unusual mechanical and transport behavior. In the machine direction it is almost elastically deformable up to strains of a few hundred percent. The elastic modulus is small as compared with the conventional polymer solid but large if compared with a normal rubber. Therefore, such are named hard elastomers. The modulus increases with decreasing temperature which is a good indication of the prevailing energetic origin of the elasticity, in contrast to the rubber with the prevailing entropic origin of the elasticity.

The hard elastomer seems to consist of lamellae oriented almost perpendicular to the extrusion direction as one expects for the row-nucleated morphology. The molecular connection between the adjacent lamellae are so localized that, upon straining, the highly recoverable accordion-type deformation takes place. The elastic bending of the free sections of lamellae between the molecular links requires, for the same bulk strain, a much smaller stress, thus yielding the low elastic modulus. It also creates a great many holes perpendicular to the strain which yield a high gas and liquid permeability, by a factor of up to 10 million higher than in the conventional solids.

## CRYSTALLIZATION FROM STIRRED OR SONICATED SOLUTION<sup>46</sup>

Since this type of crystallization will be discussed extensively during this meeting it will be surveyed here only very superficially without any ambition for completeness. The theoretical background of all phenomena observed is identical with that discussed in the above sections on crystallization from strained melts and networks. The local alignment and stretching of the initially randomly coiled macromolecules increases the dissolution and precipitation temperature and, hence, favors the crystallization, i.e. the nucleation and crystal growth, at much higher temperatures than in a solution at rest. The effects of the local stress enhancement favor the linear growth of nuclei so that the only nuclei found in stirred or sonicated solution are the long row nuclei. The existence of fibrillar elements homogenizes the local flow and reduces the gradient to such an extent that the epitaxial overgrowth of conventional lamellae can start on them.

The fibrillar nuclei are formed in the regions with a sufficiently large longitudinal gradient as, for instance, at the boundary of vortices of the turbulent flow or at the sharp edges of stirrers.<sup>47</sup> By the lamellar overgrowth one obtains the characteristic shish-kebab structure with a very long and thin central

nucleus (shish) and irregularly spaced and twisted folded-chain lamellae (kebab) of almost constant lateral dimensions irrespective of the growth time. Besides the primary nucleus one very often finds additional, longitudinal connections extending over a great many lamellae and, in many respects, appearing like parallel row nuclei. They may be microfibrils or bundles of taut tie molecules formed during crystallization or by plastic deformation, or simply parallel row nuclei held together by the rather irregular lamellar overgrowth.

The row nucleus seems again to be composed of fairly extended chains with some folds as concluded from the superheating studies and from molecular weight distribution of the fuming nitric acid etched samples. The extended-chain component of such a micro shish-kebab may be the true primary row nucleus and the folded-chain component is a dense epitaxial overgrowth deposited at an early stage of the crystallization. At the highest temperatures, about 99°C with PE in xylene, one indeed obtains only very long ( $\sim 300 \mu\text{m}$ ) and wide ( $\sim 0.5 \mu\text{m}$ ) micro shish-kebab ribbons. The relatively high elastic modulus, 20 GPa, invited the temptation to produce such fibers on a technical scale although this value was much less than that obtained by the much simpler drawing process.<sup>48,49</sup> But most recent reports claim a PE fiber formed at 119.5°C with a modulus  $E = 105 \text{ GPa}$  and a stress to break  $\sigma_f = 2.8 \text{ GPa}$ . These values substantially surpass those obtained with drawn or extruded samples.<sup>50</sup>

The growth of the primary nucleus formed from the partially aligned and extended chains by the addition of new chain elements is strongly affected by the non-vanishing velocity difference between the nucleus and the liquid. The velocity of a freely floating nucleus corresponds to the average of local liquid velocity over the whole extension of the nucleus. In a flow with a finite velocity gradient, it differs from that of most of the surrounding liquid and that more so the closer one is to the ends of the linear nucleus. The situation is still more extreme for a nucleus which is dragged through the liquid by being attached to the stirrer or to the walls of the vessel. Behind such a particle, a flow with longitudinal gradient is established which extends the coiled macromolecules and thus eases their crystallization.

The velocity difference yields a strong pulling force on the molecules already attached with one end to the nucleus but still belonging with the other end to the liquid. Such molecules do not have much chance for folding if the fold would imply the deposition of segments in the direction opposite to the pulling force. In the pulling direction, however, much longer straight sections can be deposited than in the case of crystallization from the liquid at rest. In contrast to the conventional crystallization mechanism which yields practically only primary and secondary nuclei of the minimum or slightly larger thickness and, hence, fairly constant lamella thickness, one has in the non-uniform flow

or with a dragged nucleus a strong tendency to a persistent linear growth of the nucleus in its longitudinal direction. This tendency yields the so-called row nucleus with most of the chains at least partially extended, although occasional folds are also present. The thermodynamics of such a process were described above in the section on the crystallization of a strained network.

The epitaxial overgrowth of lamellae on the row nucleus starts with much too large a lamella thickness because the chains are pulled in one direction and prevented from folding back by their sections still remaining in the liquid. This goes on as long as the velocity difference between the nucleus and the surrounding liquid is maintained. According to hydrodynamics, the difference is maximum at the ends of the linear nucleus. It decreases gradually farther away from the ends.

The progressive immobilization of the surrounding liquid by the many long row nuclei rapidly restores the conditions of crystal growth to those of the conventional crystallization from the liquid at rest with the regular chain folding and fairly constant lamella thickness. But it also limits the lateral growth of lamellae by reducing the supercooling.

## CONCLUSIONS

The reduction of the entropy of macromolecules in the strained liquid phase increases the melting point and, hence, at any temperature the effective supercooling. The simultaneous decrease of the heat content acts in the opposite direction. But its influence is always smaller than that of the entropy change. The resulting increase of the supercooling enormously enhances the rate of nucleation and crystal growth which depends exponentially on the square of the supercooling. Moreover, the anisotropy of the more or less uniaxial strain field favors the formation of linear nuclei oriented in the strain direction. Kinematic considerations of the chain deposition in a flow field with a finite velocity difference between the linear nucleus and the polymer solution corroborate this purely thermodynamic conclusion based on the local entropy changes in the strain field.

The steadily longer and more numerous row nuclei very soon carry so much of the load that the liquid between them can almost fully relax. Hence, a very modest increase of supercooling remains in contrast to the initial stage when the large increase was so conspicuously operative in the formation of the long primary row nuclei. Hence, the epitaxial overgrowth with the conventional morphology of the folded-chain lamellae can start on the linear row nuclei and proceed as long as the local supercooling permits the formation of secondary nuclei on the growth faces. The resulting lamellae of the shish-kebab or

cylindritic structure are roughly perpendicular to the initial strain and eventually helically twisted as demanded by the growth mechanism.

## References

1. B. Wunderlich, *Macromolecular Physics* (Academic Press, New York, 1976), Vol. 2.
2. J. D. Hoffman, G. T. Davis, and J. I. Lauritzen, Jr., The rate of crystallization of linear polymers with chain folding, in N. B. Hannay (Ed.), *Treatise on Solid State Chemistry* (Plenum Press, New York, 1976), Vol. 3, Chapt. 7.
3. J. D. Hoffman and J. J. Weeks, *J. Chem. Phys.* **37**, 1723 (1962).
4. R. L. Cormia, F. P. Price, and D. Turnbull, *J. Chem. Phys.* **37**, 1333 (1962).
5. G. S. Ross and L. J. Frolen, unpublished work quoted in Ref. 2.
6. H. G. Zachmann, *Kolloid-Z. Z. Polymere* **216/217**, 180 (1967).
7. H. G. Zachmann, *Kolloid-Z. Z. Polymere* **231**, 504 (1969).
8. G. T. Davis, R. K. Eby, and G. M. Martin, *J. Appl. Phys.* **39**, 4973 (1968).
9. J. I. Lauritzen, Jr. and J. D. Hoffman, *J. Appl. Phys.* **44**, 4340 (1973).
10. J. P. Arlie, P. Spegt, and A. Skoulios, *Makromol. Chem.* **104**, 212 (1967).
11. B. Wunderlich and T. Arakawa, *J. Polymer Sci.* **A2**, 3697 (1964).
12. D. C. Bassett and D. R. Carder, *Polymer* **14**, 387 (1973).
13. R. L. Miller, Status of the analysis of crystallization kinetic data, in R. L. Miller (Ed.), *Flow-Induced Crystallization (in Polymer Systems)*. (Gordon and Breach, New York, to be published in 1979), p. 31.
14. G. Allegra, *J. Chem. Phys.* **66**, 5453 (1977).
15. For more detailed information see the comprehensive article, The amount and location of amorphous component in polyethylene single crystals, by A. Peterlin, *J. Macromol. Sci.-Phys.* **B3**, 19 (1969).
16. V. F. Holland and P. H. Lindenmeyer, *J. Appl. Phys.* **36**, 3049 (1965).
17. H. Hendus, *Kolloid-Z.* **165**, 32 (1959).
18. R. Corneliussen and A. Peterlin, *Makromol. Chem.* **105**, 192 (1967).
19. G. Meinel and A. Peterlin, *Kolloid-Z. Z. Polymere* **242**, 1151 (1970).
20. T. J. Bessel and R. J. Young, *J. Polym. Sci., Polym. Letters Ed.* **12**, 629 (1974).
21. F. J. Balta-Calleja, A. Peterlin, and B. Crist, *J. Polym. Sci., Pt. A-2* **10**, 1749 (1972).
22. A. Peterlin and F. J. Balta-Calleja, *Kolloid-Z. Z. Polymere* **242**, 1093 (1970).
23. F. J. Balta-Calleja and A. Peterlin, *J. Macromol. Sci.-Phys.* **B4**, 519 (1970).
24. K. Sakaoku, N. Morosoff, and A. Peterlin, *J. Polym. Sci., Polym. Phys. Ed.* **11**, 31 (1973).
25. G. Meinel and A. Peterlin, *J. Polym. Sci., Pt. A-2* **9**, 67 (1971).
26. A. Peterlin and C. Reinhold, *J. Polym. Sci.* **A3**, 2801 (1965).
27. For references to this and subsequent sections see the special issue of *Polymer Eng. Sci.* **16/3** (1976) containing articles on Stress-induced crystallization presented at the Division of Polymer Chemistry sponsored Symposium at the American Chemical Society Meeting in Chicago, Ill., August 24-29, 1975. Also see J. N. Hay, Crystallization from the melt, in R. L. Miller (Ed.), *Flow-Induced Crystallization (in Polymer Systems)*. (Gordon and Breach, New York, to be published in 1979), p. 69.
28. K. Dušek and W. Prins, *Adv. Polymer Sci.* **6**, 1 (1969).
29. M. Katz, *Nature* **13**, 410 (1925).
30. R. Oono, K. Migasaki, and K. Ishikawa, *J. Polym. Sci., Polym. Phys. Ed.* **11**, 1477 (1973).
31. E. H. Andrews and B. Reeve, *J. Mater. Sci.* **6**, 547 (1971).
32. A. N. Gent, *J. Polym. Sci., Pt. A-2* **4**, 447 (1966).
33. I. L. Hay, M. Jaffe, and K. F. Wissbrun, *J. Macromol. Sci.-Phys.* **B12**, 423 (1976).
34. E. H. Andrews, P. J. Owen, and A. Singh, *Proc. Roy. Soc. (London)* **A324**, 79 (1971).
35. M. R. Mackley and A. Keller, *Phil. Trans. Roy. Soc. (London)* **278**, 29 (1975).
36. L. Nicodemo, G. Marucci, and J. J. Hermans, *J. Polym. Sci., Pt. A-2* **10**, 135 (1972).
37. R. Greco, G. Titomanlio, and G. Marucci, *Rheol. Acta* **13**, 532 (1974).

38. A. Keller, Lecture at the Symposium on Ultrahigh Elastic Modulus Polymers, Santa Margherita Ligure, Italy, May 23–27, 1977.
39. J. R. Dees and J. E. Spruiell, *J. Appl. Polym. Sci.* **18**, 1053 (1974).
40. J. H. Southern and R. S. Porter, *J. Macromol. Sci.-Phys.* **B4**, 541 (1970).
41. K. Imada, T. Yamamoto, K. Shigematsu, and M. Takayanagi, *J. Mater. Sci.* **6**, 537 (1971).
42. A. Keller and M. J. Machin, *J. Macromol. Sci.* **B1**, 41 (1967).
43. R. B. Williamson and W. F. Busse, *J. Appl. Phys.* **38**, 4187 (1967).
44. A. Peterlin, C. Quan, and D. T. Turner, *J. Polym. Sci.* **B3**, 521 (1965).
45. See, for instance, the review article, Hard elastic fibers, by S. L. Cannon, G. B. McKenna, and W. O. Statton, *Macromol. Rev.* **11**, 209 (1976), and H. D. Noether, this issue, p. 57 and in R. L. Miller (Ed.), *Flow-Induced Crystallization (in Polymer Systems)*. (Gordon and Breach, New York, to be published in 1979), p. 217.
46. A. J. Pennings, Crystallization under extreme temperature and pressure gradients, in R. L. Miller (Ed.), *Flow-Induced Crystallization (in Polymer Systems)*. (Gordon and Breach, New York, to be published in 1979), p. 57.
47. A. J. Pennings, *Proc. Intern. Conf. Crystal Growth* (Pergamon Press, Oxford, 1966), p. 389.
48. See, for instance, G. Meinel and A. Peterlin, *J. Polym. Sci.* **B5**, 613 (1967).
49. G. Capaccio, T. A. Crompton, and I. M. Ward, *J. Polym. Sci., Polym. Phys. Ed.* **14**, 1641 (1976).
50. A. Zwijnenburg and A. J. Pennings, *J. Polym. Sci., Polym. Letters Ed.* **14**, 338 (1976).